

Multidimensional heterogeneity learning for count value tensor data with applications to field goal attempt analysis of NBA players

Guanyu Hu*, Yishu Xue[†] and Weining Shen[‡]

May 23, 2022

Abstract

We propose a multidimensional tensor clustering approach for studying how professional basketball players' shooting patterns vary over court locations and game time. Unlike most existing methods that only study continuous-valued tensors or have to assume the same cluster structure along different tensor directions, we propose a Bayesian nonparametric model that deals with count-valued tensors and projects the heterogeneity among players onto tensor dimensions while allowing cluster structures to be different over directions. Our method is fully probabilistic; hence allows simultaneous inference on both the number of clusters and the cluster configurations. We present an efficient posterior sampling method and establish the large-sample convergence properties for the posterior distribution. Simulation studies have demonstrated an excellent empirical performance of the proposed method. Finally, an application to shot chart data collected from 191 NBA players during the 2017–2018 regular season is conducted and reveals several interesting insights for basketball analytics.

1 Introduction

There is a rapid growth in sports analytics over the recent years thanks to the fast development in game tracking technologies (Albert et al., 2017). New statistics and machine learning methods are largely needed to address a range of questions from game outcome prediction to player performance evaluation (Cervone et al., 2014; Franks et al., 2015; Cervone et al.,

*Department of Statistics, University of Missouri - Columbia

[†]Google Inc

[‡]Department of Statistics, University of California, Irvine

2016), and to in-game strategy planning (Fernandez and Bornn, 2018; Sandholtz et al., 2020).

Our focus in this paper is to study the National Basketball Association (NBA) players' *shooting patterns*, in particular, how they change over shooting locations and game time (e.g., first quarter versus clutch time). In professional basketball research, shooting pattern (or field goal attempt) is a fundamental metric since it often provides valuable insights to players, coaches and managers, e.g., players and coaches will be able to obtain a better understanding of their current shooting choices and hence develop further offensive/defensive plans accordingly, while managers can make better data-informed decisions on player recruitment. In the literature, it is common to employ spatial and spatial-temporal models (Reich et al., 2006; Miller et al., 2014; Jiao et al., 2020) to study the spatial and temporal dependence in the field goal attempt data. The key novelty of our paper is to introduce a new Bayesian tensor multidimensional clustering method that studies the heterogeneity of shooting patterns among players.

Our starting point is to recognize that the field goal attempt data in basketball games enjoys a natural *tensor structure*. For example, we can divide the basketball half court into regions under the *polar coordinate* system and then summarize the number of field goal attempts over each region during each of the four quarters of the game as entries in a three-way tensor, where each tensor direction corresponds to the shooting distance, angle, and game time (quarter). One advantage of considering a tensor representation is that the spatial-temporal dependence structure is automatically considered as part of the tensor structure. Compared to the most existing works that rely on Cartesian coordinate system (Miller et al., 2014; Jiao et al., 2020; Yin et al., 2020; Hu et al., 2020; Yin et al., 2020), our approach certainly makes more sense since shooting angle and distance are two important factors that affect the shooting selection of professional players (Reich et al., 2006). Studying the change of shooting patterns over time is also meaningful, e.g., Stephen Curry has made a comparable fewer number of attempts in fourth quarter during regular season simply because Golden State Warriors has often established a significant lead at the end of the third quarter during the 2017-2018 regular season.

Tensor models have received a great deal of attention in machine learning and statistics

literature (Kolda and Bader, 2009; Sun et al., 2014; Bi et al., 2021). For tensor clustering problems, most existing work (Sun and Li, 2019; Chi et al., 2020; Mai et al., 2021) either works with a single tensor or assumes that the clustering structure is the same across different tensor directions. It is also common that they only consider tensors with entries that takes continuous or binary values. In terms of model estimation, clustering is often based on solving a regularized optimization problem, which requires pre-specifying the number of clusters or choosing the cluster number based on certain *ad hoc* criteria. There are some recent papers on Bayesian tensor models, e.g., Guhaniyogi et al. (2017); Spencer et al. (2019); Guhaniyogi (2020). However, all of them are in the regression context, hence cannot be directly applied to solve our problem. Our proposed approach differs with aforementioned methods in several ways. First, we consider a flexible multidimensional tensor clustering problem, which allows different clustering structures over tensor directions. We believe this is a meaningful relaxation in many applications, e.g., basketball players’ shooting choice may differ significantly in terms of shooting distance, angle and game time depending on players’ position, shooting preference and role in the team. Moreover, we focus on count-valued tensors (rather than continuous-valued tensors) for the obvious reason that the number of shot attempts is the main outcome of interest in our application. Thirdly, our model is fully probabilistic, which allows an easier interpretation compared to optimization-based method. In particular, we consider a Bayesian nonparametric model under the mixture of finite mixtures framework (MFM; Miller and Harrison, 2018), which allows simultaneous estimation and inference for the number of clusters and the associated clustering configuration for each direction (e.g. distance, angle, and quarter). We show that the posterior inference can be conducted efficiently for our method and demonstrate its excellent empirical performance via simulation studies. We also establish posterior convergence properties for our method. Finally, our proposed method reveals several interesting data-driven insights of field goal attempts data which are useful for professional basketball players, coaches, and managers.

Main contributions and broad impact: (1) We are among the first (to the best of our knowledge) to introduce *tensor models* to sports analytics. It is our hope that this paper can contribute to promoting more use of tensor methods in different sport applications.

(2) We develop a novel multidimensional tensor clustering approach that allows different clustering structures over tensor directions and handles count-valued data. The proposed method is fully Bayesian, which renders convenient inference on the number of clusters and the clustering structure. (3) We provide a large-sample theoretical justification for our method by showing posterior consistency for the cluster number and contraction rate for the mixing distributions. These results are new for Bayesian tensor models.

2 Method

2.1 Probabilistic multi-dimensional tensor clustering

We treat the shooting chart data as three-way tensors and discuss a multi-dimensional clustering approach in this section. Note that each direction of the tensor represents the shooting angle, distance to the basket, and one of the four quarters in the game. Our proposed method can be conveniently extended to study general multi-way tensor data as well. Let \mathbf{Y} be a $p_1 \times p_2 \times p_3$ tensor with each element Y_{ijk} only taking count values for $i = 1, \dots, p_1; j = 1, \dots, p_2; k = 1, \dots, p_3$. It is natural to consider a Poisson distribution with a mean parameter represented as a rank-one tensor, that is,

$$\mathbf{Y} \sim \text{Poisson}(\boldsymbol{\gamma}_1 \circ \boldsymbol{\gamma}_2 \circ \boldsymbol{\gamma}_3), \quad (1)$$

where \circ denotes the outer product between two vectors, and $\boldsymbol{\gamma}_1 \in \mathbb{R}_+^{p_1}, \boldsymbol{\gamma}_2 \in \mathbb{R}_+^{p_2}, \boldsymbol{\gamma}_3 \in \mathbb{R}_+^{p_3}$. Model (1) can also be viewed as a Poisson regression model where the mean parameter corresponds to an analysis of variance (ANOVA) model with main effects only, that is, $\log \mathbb{E}(Y_{ijk}) = \log \gamma_{1,i} + \log \gamma_{2,j} + \log \gamma_{3,k}$ for $1 \leq i \leq p_1, 1 \leq j \leq p_2, 1 \leq k \leq p_3$. By ignoring the interaction effects, the number of parameters is effectively reduced from $p_1 p_2 p_3$ to $(p_1 + p_2 + p_3)$. Hence it renders parsimonious parameter estimation and easy interpretation in our NBA application study, i.e., the main effects $\log \boldsymbol{\gamma}_1, \log \boldsymbol{\gamma}_2, \log \boldsymbol{\gamma}_3$ correspond to the additive effect of shooting distance, angle, and game time (quarter).

In order to learn the multidimensional heterogeneity pattern, we consider three independent mixture of finite mixtures (MFM; Miller and Harrison, 2018) priors on $\boldsymbol{\gamma}_1, \boldsymbol{\gamma}_2, \boldsymbol{\gamma}_3$ such that the clustering pattern in those three directions can be learned separately. Here

we present a brief introduction to MFM without getting into more details. Given n observations, we consider z_1, \dots, z_n as their clustering labels, e.g., $z_1 = z_2 = z_4$ would mean that observations 1, 2, 4 belong to the same cluster. Then the MFM prior can be expressed as

$$K \sim p(\cdot), \quad (\pi_1, \dots, \pi_K) \mid K \sim \text{Dir}(\gamma, \dots, \gamma), \quad z_i \mid K, \pi \sim \sum_{h=1}^K \pi_h \delta_h, \quad i = 1, \dots, n, \quad (2)$$

where K is the number of clusters, (π_1, \dots, π_K) are associated cluster weights and $\sum_{h=1}^K \pi_h \delta_h$ is the mixture distribution with δ_h being a point-mass at h . Under the Bayesian framework, all those three quantities are random and hence are assigned with prior distributions, i.e., we use $p(\cdot)$, which is a proper probability mass function on \mathbb{N}_+ , as a prior on K , and a Dirichlet distribution on the mixture weights. Compared to the Chinese restaurant process (CRP), the probability of introducing a new table (cluster) for MFM is slowed down by a factor of $V_n(t+1)/V_n(t)$, which allows for a model-based pruning of the tiny extraneous clusters. Here the coefficient $V_n(t)$ is defined as

$$V_n(t) = \sum_{k=1}^{+\infty} \frac{k_{(t)}}{(\gamma k)^{(n)}} p(k),$$

where $k_{(t)} = k(k-1)\dots(k-t+1)$, and $(\gamma k)^{(n)} = \gamma k(\gamma k+1)\dots(\gamma k+n-1)$, and γ is the hyperparameter in the Dirichlet prior for the weights. The conditional distributions of $z_i, i = 2, \dots, n$ under (2) can be defined in a Pólya urn scheme similar to CRP:

$$P(z_i = c \mid z_1, \dots, z_{i-1}) \propto \begin{cases} |c| + \gamma, & \text{at an existing table labeled } c \\ V_n(t+1)/V_n(t)\gamma, & \text{if } c \text{ is a new table} \end{cases}, \quad (3)$$

with t being the number of existing clusters.

Now back to the shooting chart data, as we propose to use three independent MFM priors for clustering shooting distance, angle, and game time, our final model can be presented in

the following hierarchical structure,

$$\begin{aligned}
K_\ell &\stackrel{\text{i.i.d.}}{\sim} p_K, \quad \ell = 1, 2, 3, \\
\boldsymbol{\pi}_\ell &= (\pi_{\ell,1}, \dots, \pi_{\ell,K_\ell}) \mid K_\ell \sim \text{Dir}(\nu, \dots, \nu), \quad \nu > 0, \quad \ell = 1, 2, 3, \\
\log \boldsymbol{\gamma}_{\ell,1}, \dots, \log \boldsymbol{\gamma}_{\ell,K_\ell} &\stackrel{\text{i.i.d.}}{\sim} \text{MVN}_{p_\ell}(\mathbf{0}, \boldsymbol{\Sigma}_\ell), \quad \ell = 1, 2, 3, \\
\boldsymbol{\Sigma}_\ell &= \sigma_\ell^2 (I_\ell - \rho_\ell \mathbf{W}_\ell), \quad \ell = 1, 2, 3, \\
\sigma_\ell^2 &\sim \text{Gamma}(a, b), \quad \ell = 1, 2, 3, \\
\rho_\ell &\sim \text{Unif}(c_{1\ell}, c_{2\ell}), \quad \ell = 1, 2, 3, \\
P(z_{i\ell} = j \mid \boldsymbol{\pi}_\ell, K_\ell) &= \pi_{j\ell}, \quad \ell = 1, 2, 3, \quad j = 1, \dots, K_\ell, \\
\mathbf{Y}_i &\sim \text{Poisson}(\boldsymbol{\gamma}_{1,z_{i1}} \circ \boldsymbol{\gamma}_{2,z_{i2}} \circ \boldsymbol{\gamma}_{3,z_{i3}}), \quad i = 1, \dots, n,
\end{aligned} \tag{4}$$

where the main effects for distance, angle, and period are modeled by multivariate normal distributions and their covariance matrices involve adjacency matrices, denoted by \mathbf{W}_ℓ 's, that are used for incorporating the potential spatial and temporal correlation information (e.g., two shooting locations are next to each other). To ensure those covariance matrices $\boldsymbol{\Sigma}_\ell$ are positive definite, we introduce $c_{1\ell}$ and $c_{2\ell}$ as the reciprocals of minimum and maximum eigenvalues of \mathbf{W}_ℓ , respectively. For the prior p_K on the number of clusters, we consider a truncated Poisson(1) following the recommendations in Miller and Harrison (2018) and Geng et al. (2019).

Our multidimensional clustering model in (4) sits between two extremes. One is the usual tensor clustering model that assumes the same cluster structure across different directions, which certainly is more restrictive compared to ours. The other is to marginally cluster over each of the tensor directions and solve multiple clustering problems independently, which does not fully utilize the tensor structural information. Our method combines the attractive features from both sides by allowing cluster structures to be different over directions while borrowing information to improve the estimation efficiency.

Our model in (4) can be viewed as a Bayesian mixture of rank-one tensor models. Compared to the frequentist work on tensor clustering (Sun and Li, 2019; Chi et al., 2020), where a Tucker decomposition is usually utilized and the choice of the rank relies heavily on pre-specification or certain model selection criteria, our approach is capable of automatically determining the rank while quantifying the uncertainty in rank selection. Moreover, our

method is fully probabilistic; hence each mixture component is easy to interpret in practice.

2.2 Theoretical Properties

Next we study the theoretical properties for the posterior distribution obtained from model (4). For convenience, we define three mixing measures $G_\ell = \sum_{i=1}^{K_\ell} \pi_{\ell,i} \delta(\gamma_{\ell,i})$ for $\ell = 1, 2, 3$, where $\delta(\cdot)$ is the point mass measure. In other words, G_1, G_2, G_3 represent the clustering structures and associated parameters along each of the three directions in the tensor. In order to establish the posterior contraction results, we consider a refined parameter space Θ^* defined as $\cup_{k_1, k_2, k_3=1}^{\infty} \Theta_{\mathbf{k}}^*$ for $\mathbf{k} = (k_1, k_2, k_3)$, where $\Theta_{\mathbf{k}}^*$ is a compact parameter space for all model parameters including mixture weights and main effects given a fixed cluster number for each direction, i.e., $K_1 = k_1, K_2 = k_2$, and $K_3 = k_3$. More precisely, we define $\Theta_{\mathbf{k}}^*$ as

$$\left\{ \begin{array}{l} \pi_{\ell,i} \in (\epsilon, 1 - \epsilon) \text{ for every } i = 1, \dots, k_\ell, \ell = 1, 2, 3, \quad \sum_j^{k_\ell} \pi_{\ell,j} = 1 \text{ for every } \ell = 1, 2, 3, \\ \gamma_{\ell,i} \in (-M, M) \text{ for every } i = 1, \dots, k_\ell, \ell = 1, 2, 3, \end{array} \right\},$$

where ϵ and M are some pre-specified positive constants. For any two mixing measures $G_1 = \sum_{i=1}^k p_i \delta(\gamma_i)$ and $G_2 = \sum_{j=1}^{k'} p'_j \delta(\gamma_j)$, we define their Wasserstein distance as $W(G_1, G_2) = \inf_{q \in \mathcal{Q}} \sum_{i,j} q_{ij} |\gamma_i - \gamma_j|$, where \mathcal{Q} denotes the collection of joint discrete distribution on the space of $\{1, \dots, k\} \times \{1, \dots, k'\}$ and q_{ij} is the probability being associated with (i, j) -element and it satisfies the constraint that $\sum_{i=1}^k q_{ij} = p'_j$ and $\sum_{j=1}^{k'} q_{ij} = p_i$, for every $i = 1, \dots, k$ and $j = 1, \dots, k'$.

For $\ell = 1, 2, 3$, let K_ℓ^0 and G_ℓ^0 be the true number of clusters and true mixing measure along direction ℓ . Also let P_0 be the associated joint probability measure. Then the following theorem establishes the posterior consistency and contraction rate for the cluster number and mixing measure. The proof is given in the Supplementary Material; and it is based on the results for Bayesian mixture models in Guha et al. (2021).

Theorem 1. *Let $\Pi_n(\cdot \mid \mathbf{Y}_1, \dots, \mathbf{Y}_n)$ be the posterior distribution obtained from (4) given i.i.d. observations $\mathbf{Y}_1, \dots, \mathbf{Y}_n$. Suppose that the true parameters belong to Θ^* . Then for*

each of $\ell = 1, 2, 3$, we have

$$\Pi_n \{K_\ell = K_\ell^0 \mid \mathbf{Y}_1, \dots, \mathbf{Y}_n\} \rightarrow 1, \text{ and } \Pi_n \{(W(G_\ell, G_\ell^0) \lesssim (\log n/n)^{-1/2} \mid \mathbf{Y}_1, \dots, \mathbf{Y}_n)\} \rightarrow 1,$$

almost surely under P_0 as $n \rightarrow \infty$.

Theorem 1 shows that as sample size $n \rightarrow \infty$, our proposed Bayesian model is capable of correctly identifying the unknown number of clusters along each of the tensor directions with posterior probability tending to one. Moreover, the latent clustering structure (e.g., cluster membership) can also be consistently recovered. The contraction rate for G_ℓ is nearly parametric with an additional logarithmic factor, which is common in the Bayesian asymptotic literature (Guha et al., 2021). The assumption of a compact parameter space Θ^* is needed to rule out extreme scenarios, for example, when some mixture probabilities are extremely close to 0, for which it becomes very challenging to distinguish between our model and a sub-model without these small mixture components. In practice, this assumption is often satisfied since we can always restrict the modeling parameters to take values within a pre-specified range, e.g., assuming cluster probability to be at least ϵ for some small ϵ values such as .0001%. Our results can also be extended to general multi-way tensors as long as the independent MFM priors are used for each direction.

2.3 Bayesian Inference

We discuss the posterior sampling scheme for our model. For the MFM prior, we use the stick-breaking (Sethuraman, 1994) approximation to reconstruct

$$K_\ell \sim p_K, \boldsymbol{\pi}_\ell = (\pi_{1\ell}, \dots, \pi_{K_\ell\ell}) \mid K_\ell \sim \text{Dir}(\nu, \dots, \nu), \quad \ell = 1, 2, 3,$$

as follows for each of $\ell = 1, 2, 3$,

- **Step 1.** Generate $\eta_1, \eta_2, \dots \stackrel{\text{iid}}{\sim} \text{Exp}(\psi_\ell)$,
- **Step 2.** Let $K_\ell = \min\{j : \sum_{k=1}^j \eta_k \geq 1\}$,
- **Step 3.** Set $\pi_{h\ell} = \eta_h$, for $h = 1, \dots, K_\ell - 1$,
- **Step 4.** Set $\pi_{h\ell} = 1 - \sum_{h=1}^{K_\ell-1} \pi_h$,

where we choose $(K_\ell - 1) \sim \text{Poisson}(\psi_\ell)$ and $\nu = 1$. Based on the stick-breaking reparameterization, we obtain a similar hierarchical model as the Dirichlet process mixture model in Ishwaran and James (2001) when we choose a sufficiently large dimension T for $\boldsymbol{\pi}_\ell$ and set the last $T - K_\ell$ elements to be zero. Due to the lack of available analytical form for the posterior distribution of γ 's, we employ the MCMC sampling algorithm to sample from the posterior distribution, and then obtain the posterior estimates of the unknown parameters. Computation is facilitated by the **nimble** (de Valpine et al., 2017) package in R (R Core Team, 2013).

To determine the final clustering configuration based on post-burn-in iterations, we use the Dahl's method (Dahl, 2006). The main idea is to obtain a clustering configuration that best represents the posterior samples based on comparing the "pairwise similarity" between different cluster structures. The procedure can be described as follows. First, at MCMC iteration t , based on the n -dimensional vector $(z_1^{(t)}, \dots, z_n^{(t)})$ for the latent clusters, a membership matrix $M^{(t)}$ consisting of 0 and 1's can be obtained, where $M^{(t)}(i, j) = M^{(t)}(j, i) = 1(z_i^{(t)} = z_j^{(t)})$. Next, the membership matrices are averaged over all post-burn-in iterations to get a matrix of pairwise similarity, $\bar{M} = \sum_{t=1}^T M^{(t)}/T$, where T denotes the total number of iterations. Finally, the iteration that has the smallest element-wise Euclidean distance from \bar{M} is taken as the inferred clustering configuration, i.e., with t^* being

$$t^* = \arg \min_t \sum_{i=1}^n \sum_{j=1}^n (M^{(t)}(i, j) - \bar{M}(i, j))^2,$$

and the final inferred configuration is obtained as $(z_1^{t^*}, \dots, z_n^{t^*})$.

3 Simulation

To evaluate the performance of the proposed model, simulation studies are performed on generated data sets with a total of 150 players. We consider two simulation settings. For the first setting, we consider a three-angle pattern and three-distance partition of the court, i.e., the court is divided into 9 parts based on combinations of distance and angle. Two clusters of size 75 are set for angle, distance, and quarter, respectively. The patterns for angle and group are visualized in Figure 8 of the Supplementary Material. For quarter group 1, we

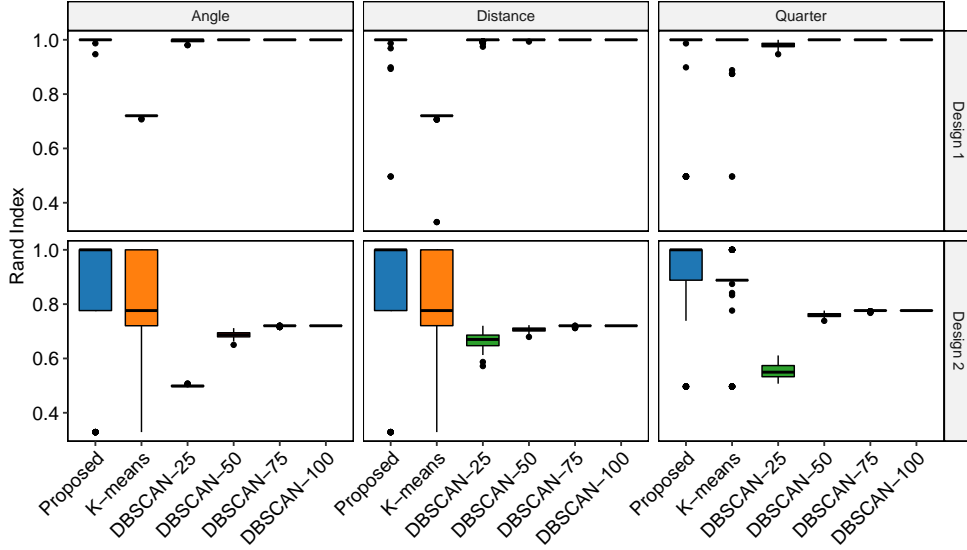


Figure 1: Simulation results: Rand index boxplots for angle, distance, and quarter over 100 Monte-Carlo replicates.

choose $\gamma_3 = (-1, -1, -1, -1)^\top$; and for quarter group 2, $\gamma_3 = (-0.5, -2, -0.5, -2)^\top$. For the second simulation setting, we consider a finer partition of the court, including 11 angles, 12 distances, and again two quarter patterns in the same way as design 1. The true number of clusters is 3 (each cluster cluster of size 50) for the angle, 3 (each cluster of size 50) for the distance, and 2 (each of size 75) for the quarter. The angle and group patterns are visualized in Figure 9 of the Supplementary Material. Under both settings, for each piece of the partitioned court, the corresponding number of shots is generated using the associated γ_1, γ_2 and γ_3 based on the last line of Equation 4. The proposed multidimensional clustering approach is then applied to fit the generated data; and this procedure is repeated for 100 times for each setting. All the computations were performed on a computing server (256GB RAM, with 8 AMD Opteron 6276 processors, operating at 2.3 GHz, with 8 processing cores in each) and the running time was within twelve hours.

To evaluate the clustering performance on each of the tensor directions, we use the Rand index (RI; Rand, 1971), which is a commonly used metric that measures the concordance between two clustering schemes. Taking values between 0 and 1, a larger value of RI indicates a higher agreement. To evaluate whether the true number of clusters is correctly inferred, we also examine the total number of clusters inferred in each replicate over each of

the three directions.

We consider two competing methods, K -means (function `kmeans()` in R) and density-based spatial clustering (DBSCAN; implemented in `fpc`, Hennig, 2020). To make a fair comparison, we use the number of clusters obtained by our method for K -means. For DBSCAN, as the method depends on a pre-specified “reachability distance”, we use four candidate values, 25, 50, 75, and 100; and we denote the methods as DBSCAN-25, . . . , DBSCAN-100 for the rest of this paper. Both methods are applied to each of the three directions in an independent manner. In other words, for 150 simulated players, we sum out the distance and quarter directions, and obtain 150 11-dimensional count vectors for clustering.

We summarize the rand indexes from 100 replicates as boxplots in Figure 1 and also report the average RI in Table 1. From the results, we find a clear advantage of our method over K -means. Compared to DBSCAN, our advantage is not obvious under the simple setting, Design 1; but becomes significantly better under Design 2. We also note that the performance of DBSCAN is quite sensitive to the choice of the reachability distance, e.g., DBSCAN-25 has the worst performance for all three directions under Design 2, but not for Design 1. Our method, on the other hand, manages to achieve a reasonably high average Rand Index for different tensor directions under both simulation designs. These results highlight the benefit of incorporating the tensor structure and borrowing information from other directions by our method.

We also present the histogram of the estimated number of clusters from 100 replicates in Figure 2. Under Design 1, where there are only two clusters on each direction, the proposed method manages to correctly estimate the cluster number 98%, 94%, and 87% of times for angle, distance, and quarter, respectively. In Design 2, with a finer partition of the court, it becomes harder to infer the number of clusters, and the percentage of correct estimation reduces to 56%, 60%, and 61%.

4 NBA Data Analysis

We consider the shot attempts made by players during the 2017–2018 NBA regular season excluding the overtime period. Rookie year players who started their NBA career in 2017

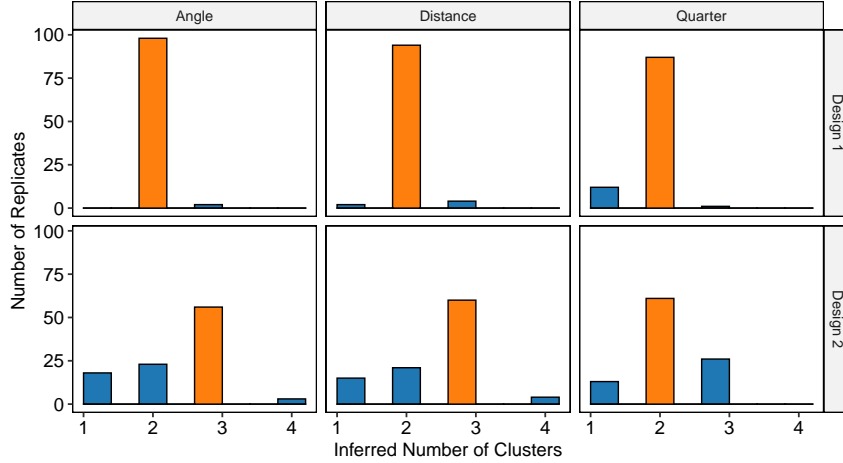


Figure 2: Simulation results: Histograms of cluster numbers over 100 Monte-Carlo replicates for angle, distance, and quarter under two designs. Correct estimate of K is marked in orange color.

Table 1: Simulation results: Average Rand Index over 100 Monte-Carlo replicates under two simulation designs for the proposed method and two competing methods.

Design	Method	Angle	Distance	Quarter
Design 1	Proposed	0.999	0.987	0.938
	K -means	0.720	0.712	0.985
	DBSCAN-25	0.996	0.998	0.982
	DBSCAN-50	1.000	1.000	1.000
	DBSCAN-75	1.000	1.000	1.000
	DBSCAN-100	1.000	1.000	1.000
Design 2	Proposed	0.826	0.851	0.903
	K -means	0.773	0.786	0.851
	DBSCAN-25	0.499	0.667	0.554
	DBSCAN-50	0.687	0.706	0.759
	DBSCAN-75	0.720	0.720	0.776
	DBSCAN-100	0.720	0.720	0.776

are excluded. We also exclude players who made very few number of shots in that season, e.g., due to long-term injury. Shots that were made at negative degrees (under the polar coordinate system) are also excluded. At the end, the dataset that we study consists of 122,001 shot attempts made by 191 players, with Aron Baynes bottoming the list with 317, and Russell Westbrook topping the list with 1356 shot attempts.

We consider the polar coordinate representation of shot attempts in a similar way with Reich et al. (2006). We treat the basket as origin and partition the angle (from 0 to π) into 11 equal sections. In terms of the shooting distance, we partition it into 12 sections, with the first 11 be designed so that the areas of all sectors and annular sectors are the same. The remaining 9 areas correspond to the remaining areas on the offensive half court. The partition scheme is illustrated in Figure 7 of the Supplementary Material. Compared to the partition scheme in Figure 2 of Reich et al. (2006), where the annular sectors only covered the regions near the three-point line, we extend the annular sectors because of the current trend of making three-point shots among NBA players, e.g., Stephen Curry and Damian Lillard. For each player, we further divide the number of shot attempts by four game quarters for each court partition, and end up with a $11 \times 12 \times 4$ -dimensional tensor. In Figure 3, we choose three players, Bradley Beal, LeBron James, and Russel Westbrook, and present their shot charts for demonstration. Some interesting patterns can be observed from the plots, e.g., LeBron James makes more shots facing the basket, and Russel Westbrook makes fewer shot attempts in the fourth quarter on average.

We apply the proposed multidimensional heterogeneity learning approach on the collected tensor data from 191 players. The same neighborhood matrices W_1 , W_2 , and W_3 from the simulation studies are used. We consider a MCMC chain of length 10,000 and a thinning interval of 2, resulting in a total of 5,000 posterior samples. We then discard the first 2,000 as burn-in and use the rest of 3,000 samples to obtain the final clustering configuration using Dahl’s method as described in Section 2.3.

We obtain two clusters of sizes 71 and 120 over the angle direction as shown in Figure 4. While it can be seen that players in both clusters make more shots when facing the basket, those in cluster 1 also make a fair amount of shots at the two wings, as well as the corners. Players in cluster 2, however, mostly shoot in the region facing the basket and its immediate

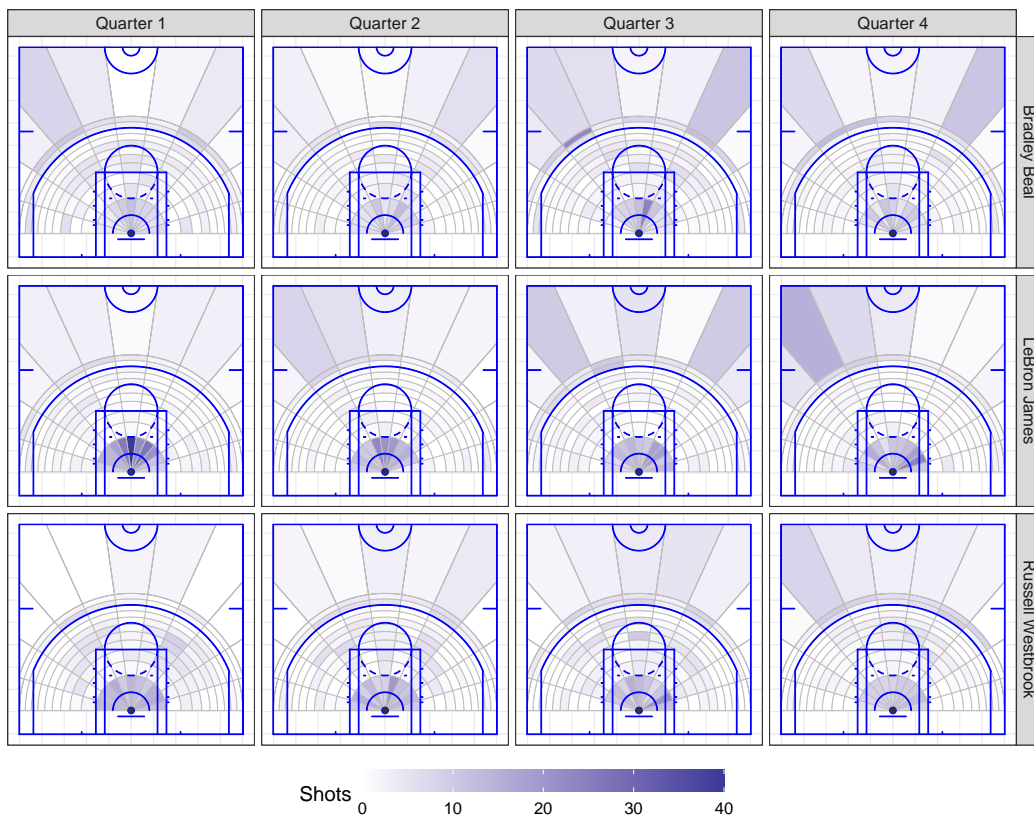


Figure 3: Visualization of shot count tensors for Bradley Beal, LeBron James, and Russell Westbrook.

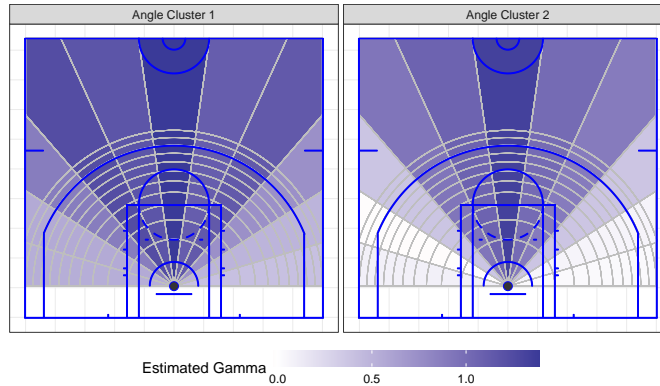


Figure 4: Visualization of γ_1 estimates for two shooting angle clusters.

neighbors. Compared to those in cluster 1, they make less corner shots, as the estimated γ_1 is almost 0 in the two regions on each side. Representative players for the two clusters are, respectively, James Harden and John Wall. Their shot charts are given in Figure 10 of the Supplementary Material.

Shooting patterns in terms of distance to basket have been clustered into three groups as visualized in Figure 5. Players in the cluster 1 have two hot regions: near the basket, and beyond the three point line. Point guards and shooting guards (small forwards) make the majority of this cluster (75 players), with representative players such as Kyrie Irving and Stephen Curry. Compared with cluster 1, the 90 players in cluster 2 tend to shoot less beyond the three point line, but make more perimeter shots. A representative player for this cluster is Russell Westbrook. Finally, in cluster 3, most of the 26 players only shoot in regions that are closest to the basket, such as DeAndre Jordan and Clint Capela. Most of their shots are slam dunks and alley-oops. Some other players (e.g., Fred VanVleet and Jonas Valanciunas) in cluster 3, although also making perimeter shots and three-pointers, rely heavily on lay-ups. We pick one representative player from each cluster and present their shooting charts in Figure 11 of the Supplementary Material.

Finally, the two clusters for quarters are visualized in Figure 6. In cluster 1, players make more shots in quarters 1 and 3, and less shots in quarters 2 and 4. Most players in this cluster are leading players in their teams, and they often take breaks during the second quarter. In the fourth quarter, leading players may also take breaks if their teams lead or fall behind by wide margins. Stephen Curry, Kevin Durant and Paul George are in this

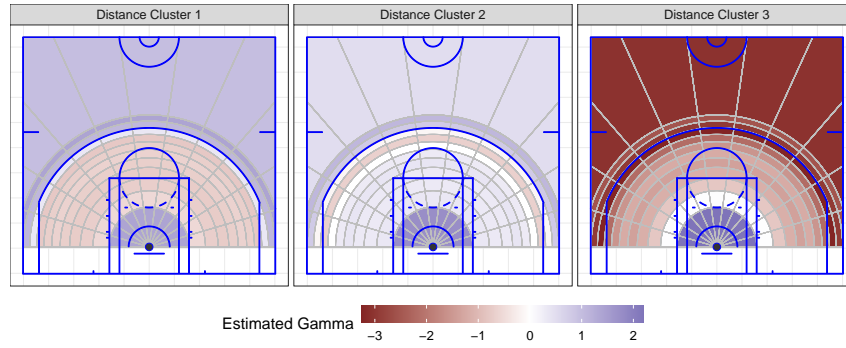


Figure 5: Visualization of γ_2 estimates for the three shooting distance clusters.

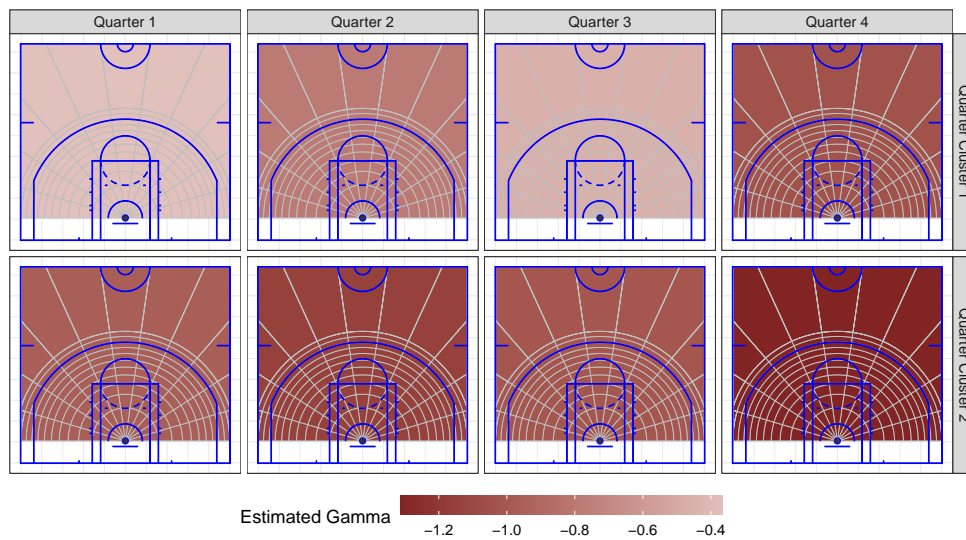


Figure 6: Visualization of γ_3 estimates for two game quarter clusters.

cluster. In cluster 2, the distribution of shots across four quarters is more even than that in cluster 1, and on average the estimated γ_3 is relatively smaller. The cluster sizes are 91 and 100, which indicate these two patterns are similarly prevalent among the players that we studied. We pick Anthony Davis and Chris Paul as two representative players from two clusters and present their shooting charts over four quarters in Figure 12 of the Supplementary Material.

5 Discussion

We propose a new multidimensional tensor clustering method in this paper and demonstrate its utility by studying how shooting patterns distribute over court locations and game time among different players. Our method is applicable to many other sports such as football and baseball, where it is natural to formulate and model the multi-way array data. The proposed method also applies to other applications such as imaging analysis and recommender systems.

Several future work directions remain open. First, our method is based on Poisson distribution for outcomes in the tensor; and it is of interest to generalize this assumption by considering other types of distributions such as zero-inflated Poisson and continuous distributions. Incorporating sparsity in tensor models is another interesting direction that will allow us to deal with high-dimensional tensors. From applications point of view, it is of interest to analyze and compare the shooting patterns between different periods of games/seasons, e.g., regular season versus playoff games, and before-pandemic versus 2020 NBA bubble seasons.

References

- Albert, J., M. E. Glickman, T. B. Swartz, and R. H. Koning (2017). *Handbook of statistical methods and analyses in sports*. CRC Press.
- Bi, X., X. Tang, Y. Yuan, Y. Zhang, and A. Qu (2021). Tensors in statistics. *Annual review of statistics and its application* 8, 345–368.
- Cervone, D., A. D’Amour, L. Bornn, and K. Goldsberry (2014). Pointwise: Predicting points and valuing decisions in real time with nba optical tracking data. In *Proceedings of the 8th MIT Sloan Sports Analytics Conference, Boston, MA, USA*, Volume 28, pp. 3.
- Cervone, D., A. D’Amour, L. Bornn, and K. Goldsberry (2016). A multiresolution stochastic process model for predicting basketball possession outcomes. *Journal of the American Statistical Association* 111(514), 585–599.

- Chi, E. C., B. R. Gaines, W. W. Sun, H. Zhou, and J. Yang (2020). Provable convex co-clustering of tensors. *Journal of Machine Learning Research* 21(214), 1–58.
- Dahl, D. B. (2006). Model-based clustering for expression data via a Dirichlet process mixture model. In M. V. Kim-Anh Do, Peter Müller (Ed.), *Bayesian Inference for Gene Expression and Proteomics*, Volume 4, pp. 201–218. Cambridge University Press.
- de Valpine, P., D. Turek, C. J. Paciorek, C. Anderson-Bergman, D. T. Lang, and R. Bodik (2017). Programming with models: writing statistical algorithms for general model structures with NIMBLE. *Journal of Computational and Graphical Statistics* 26(2), 403–413.
- Fernandez, J. and L. Bornn (2018). Wide open spaces: A statistical technique for measuring space creation in professional soccer. In *Sloan Sports Analytics Conference*, Volume 2018.
- Franks, A., A. Miller, L. Bornn, K. Goldsberry, et al. (2015). Characterizing the spatial structure of defensive skill in professional basketball. *The Annals of Applied Statistics* 9(1), 94–121.
- Geng, J., A. Bhattacharya, and D. Pati (2019). Probabilistic community detection with unknown number of communities. *Journal of the American Statistical Association* 114(526), 893–905.
- Guha, A., N. Ho, and X. Nguyen (2021). On posterior contraction of parameters and interpretability in bayesian mixture modeling. *Bernoulli* 27(4), 2159–2188.
- Guhaniyogi, R. (2020). Bayesian methods for tensor regression. *Wiley StatsRef: Statistics Reference Online*, 1–18.
- Guhaniyogi, R., S. Qamar, and D. B. Dunson (2017). Bayesian tensor regression. *The Journal of Machine Learning Research* 18(1), 2733–2763.
- Hennig, C. (2020). *fpc: Flexible Procedures for Clustering*. R package version 2.2-9.
- Hu, G., H.-C. Yang, and Y. Xue (2020). Bayesian group learning for shot selection of professional basketball players. *Stat*, e324.

- Ishwaran, H. and L. F. James (2001). Gibbs sampling methods for stick-breaking priors. *Journal of the American Statistical Association* 96(453), 161–173.
- Jiao, J., G. Hu, and J. Yan (2020). A Bayesian joint model for spatial point processes with application to basketball shot chart. *Journal of Quantitative Analysis in Sports*. Forthcoming.
- Kolda, T. G. and B. W. Bader (2009). Tensor decompositions and applications. *SIAM review* 51(3), 455–500.
- Mai, Q., X. Zhang, Y. Pan, and K. Deng (2021). A doubly-enhanced EM algorithm for model-based tensor clustering. *Journal of the American Statistical Association* (just-accepted), 1–44.
- Miller, A., L. Bornn, R. Adams, and K. Goldsberry (2014). Factorized point process intensities: A spatial analysis of professional basketball. In E. P. Xing and T. Jebara (Eds.), *Proceedings of the 31st International Conference on Machine Learning*, Volume 32 of *Proceedings of Machine Learning Research*, Beijing, China, pp. 235–243. PMLR.
- Miller, J. W. and M. T. Harrison (2018). Mixture models with a prior on the number of components. *Journal of the American Statistical Association* 113(521), 340–356.
- R Core Team (2013). *R: A Language and Environment for Statistical Computing*. Vienna, Austria: R Foundation for Statistical Computing.
- Rand, W. M. (1971). Objective criteria for the evaluation of clustering methods. *Journal of the American Statistical Association* 66(336), 846–850.
- Reich, B. J., J. S. Hodges, B. P. Carlin, and A. M. Reich (2006). A spatial analysis of basketball shot chart data. *The American Statistician* 60(1), 3–12.
- Sandholtz, N., J. Mortensen, and L. Bornn (2020). Measuring spatial allocative efficiency in basketball. *Journal of Quantitative Analysis in Sports* 16(4), 271–289.
- Sethuraman, J. (1994). A constructive definition of Dirichlet priors. *Statistica Sinica*, 639–650.

- Spencer, D., R. Guhaniyogi, and R. Prado (2019). Bayesian mixed effect sparse tensor response regression model with joint estimation of activation and connectivity. *arXiv preprint arXiv:1904.00148*.
- Sun, W. W., B. Hao, and L. Li (2014). Tensors in modern statistical learning. *Wiley StatsRef: Statistics Reference Online*, 1–25.
- Sun, W. W. and L. Li (2019). Dynamic tensor clustering. *Journal of the American Statistical Association* 114(528), 1894–1907.
- Yin, F., G. Hu, and W. Shen (2020). Analysis of professional basketball field goal attempts via a Bayesian matrix clustering approach. *arXiv preprint arXiv:2010.08495*.
- Yin, F., J. Jiao, G. Hu, and J. Yan (2020). Bayesian nonparametric estimation for point processes with spatial homogeneity: A spatial analysis of NBA shot locations. *arXiv preprint arXiv:2011.11178*.

Supplemental Material

We present additional figures referenced in the main paper.

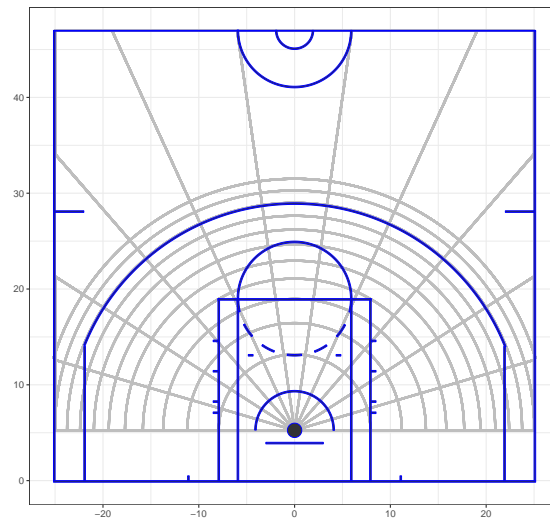


Figure 7: Illustration of the partition scheme imposed on the court.

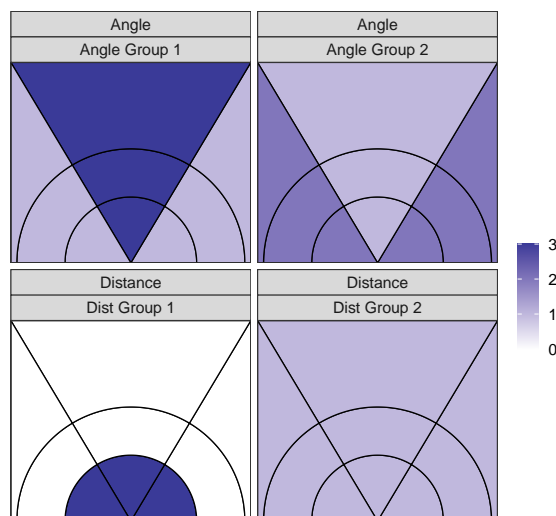


Figure 8: Visualization for γ_1 and γ_2 in the first simulation setting.

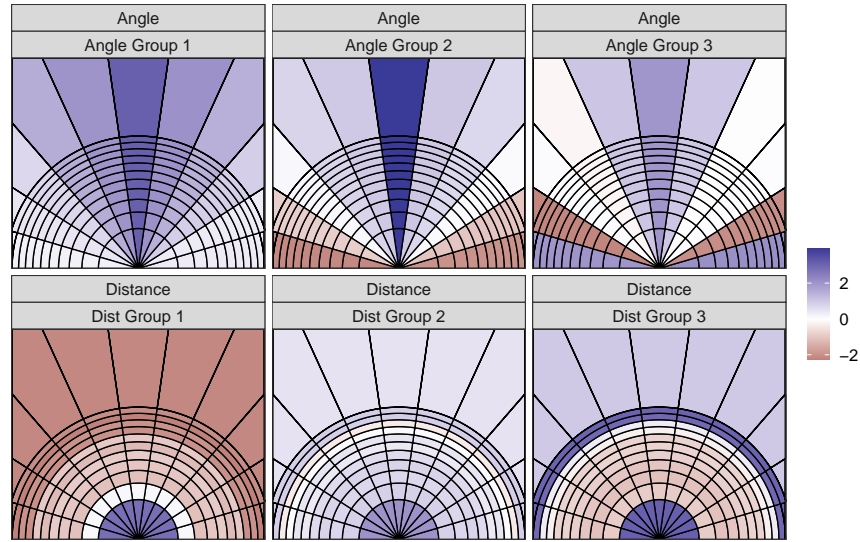


Figure 9: Visualization for γ_1 and γ_2 in the second simulation setting.

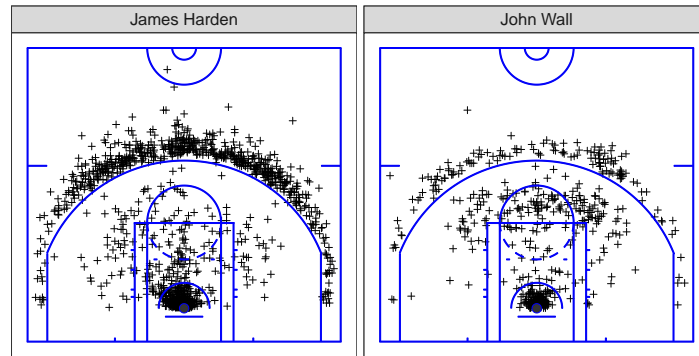


Figure 10: Shot charts for representative players from the two angle clusters.

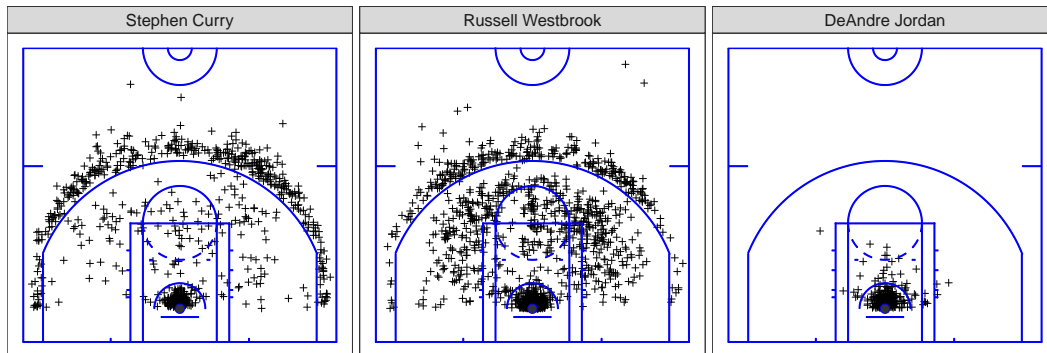


Figure 11: Shot charts for representative players from the three distance clusters.

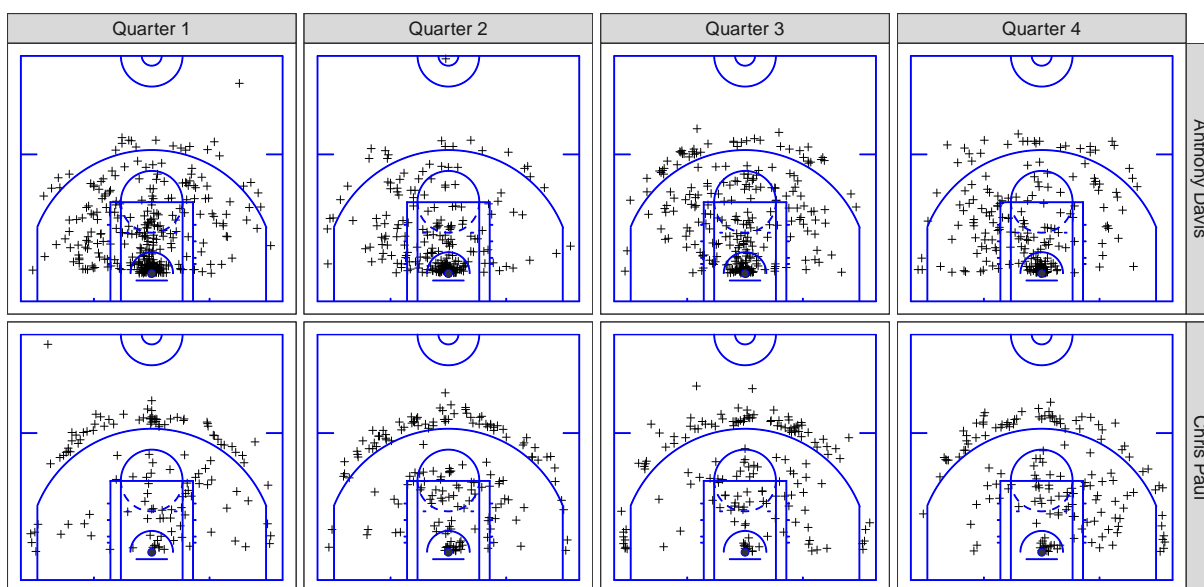


Figure 12: Shot charts for representative players from the two quarter clusters.

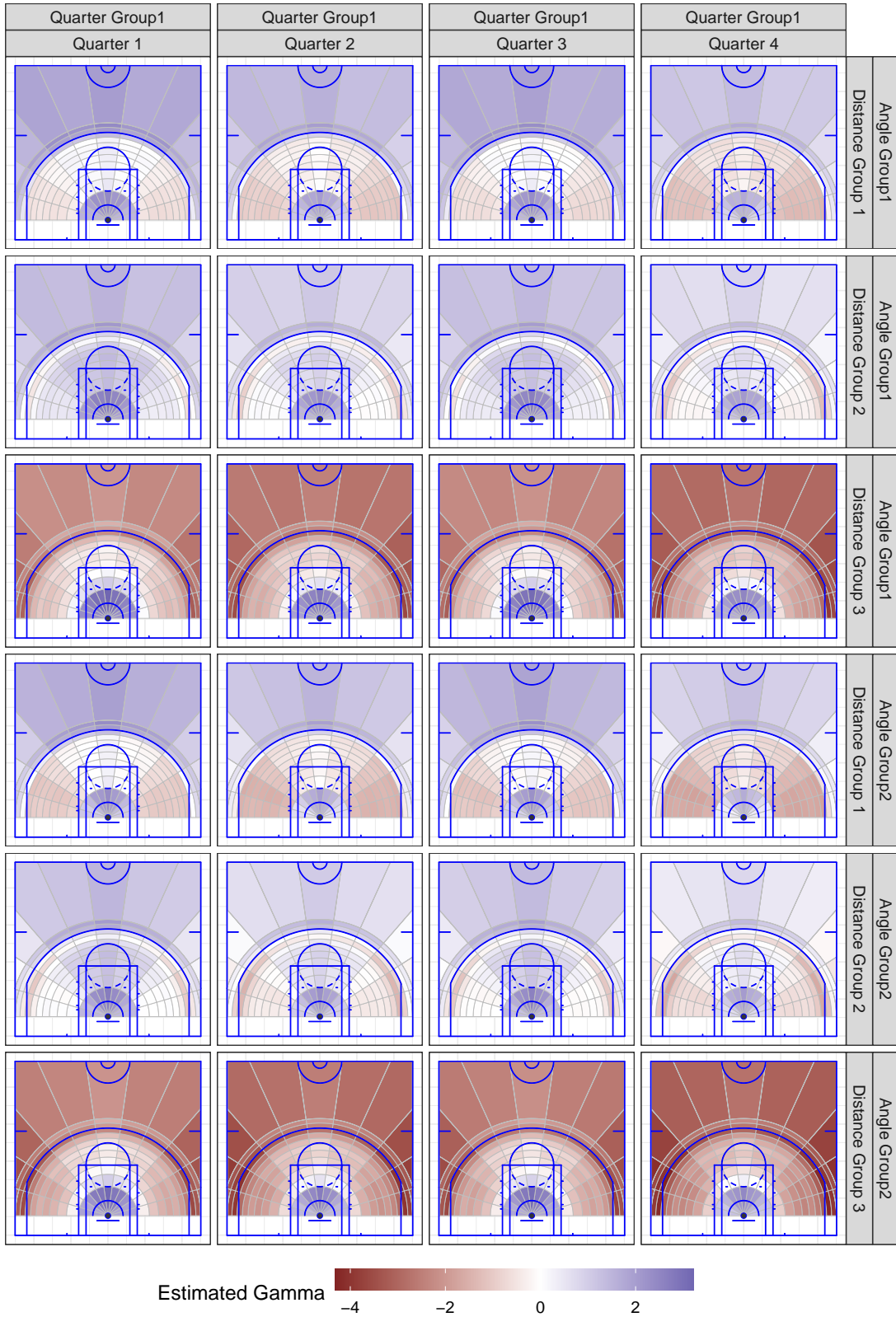


Figure 13: Visualization of $\hat{\gamma}_1 + \hat{\gamma}_2 + \hat{\gamma}_3$ for players in different distance and angle groups and quarter group 1.

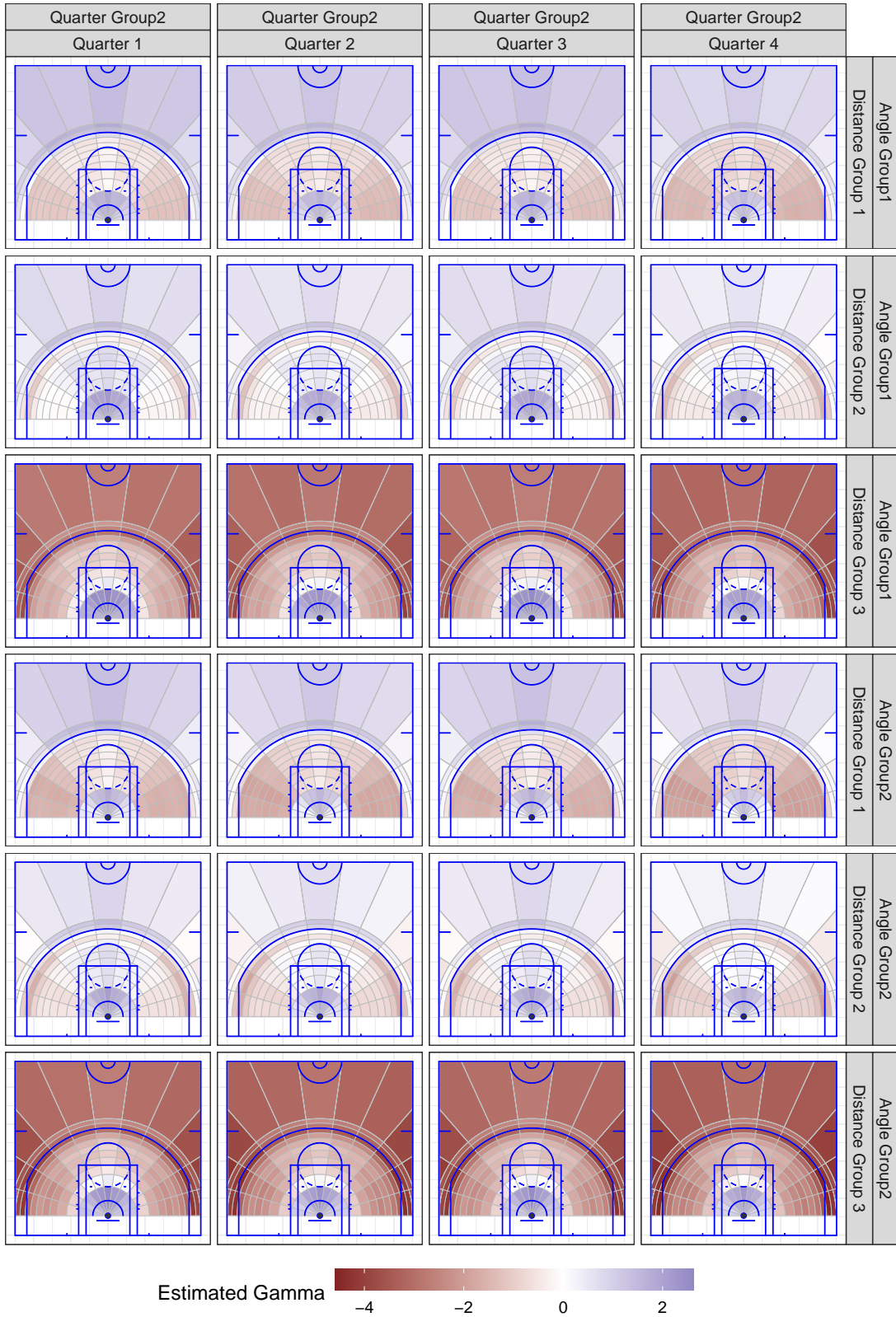


Figure 14: Visualization of $\hat{\gamma}_1 + \hat{\gamma}_2 + \hat{\gamma}_3$ for players in different distance and angle groups and quarter group 2.